Optimization of multi-function integrated optics chip fabricated by proton exchange in LiNbO$_3$

S.M. Kostritskii[1], Yu.N. Korkishko, V.A. Fedorov

RPC Optolink, Sosnovaya al.,d. 6A, str.2, NPL-3-1, Zelenograd, Moscow, 124489, Russia;

ABSTRACT

Multi-function integrated optics chips consisting of a linear polarizer, phase electro-optic modulators and Y-branching power divider were fabricated in x-cut LiNbO$_3$ wafers with the aid of annealed proton exchange technique. Insertion losses, power transfer coefficient, splitting ratio and its spectral dependence were measured for Y-branching power dividers of different branching topologies based on channel waveguides. The parasitic spectral selectivity and photorefractive damage were suppressed by optimization of branching topology, introducing an extra taper with variable parameters.

Keywords: lithium niobate, proton exchange, optical waveguide, power divider, photorefractive damage.

1. INTRODUCTION

Optical channel waveguides in lithium niobate are very useful elements for building a variety of integrated optical components. For example, the key component of fiber optical gyroscope (FOG) is the multi-function integrated optics chip (MIOC), which is an important part of the Sagnac interferometer[1]. Proton exchange (PE) is now an established technique for fabricating integrated optical devices in LiNbO$_3$ and offers possibility of obtaining low-loss MIOC[2,3]. As the MIOC consists inherently an Y-branching power divider, the wavelength sensitivity of Y-branching can present the dramatic problem if uncertainty of the light source centre wavelength is sufficient to induce marked variations in the mode coupling between two channel waveguides in branching region. Moreover, suppression of parasitic spectral selectivity is rather difficult task for real devices because of inherent asymmetry of Y-branching region, appearing due to technological uncertainty of photolithography and etching processes[3-5]. Thus, a careful design of the Y-branching is mandatory to obtain high performance devices and this means to make optimisation of Y-branching topology. We report on a specially designed Y-branching topology based on mode shaping. This design is easy to apply in technological processing and highly reproducible at industrial level in particular for lithium niobate integrated-optical devices.

2. EXPERIMENTAL

A series of power dividers utilizing the different geometries of Y-branching and straight channel guides were delineated in X-cut LiNbO$_3$ substrates, using standard photolithographic technique. The channel width W of waveguides forming an Y-branching was varied in the range from 5.6 to 6.2 µm, where formation of a low-loss single mode channel waveguide, operating within a wavelength region from 1500 to 1580 nm, is expected[3,6].

To fabricate these waveguide structures with the aid of the annealed proton-exchanged (APE) technique, the substrates were proton exchanged at 175 °C for 50÷70 min in pure benzoic acid and annealed at 360 °C for 6÷7.5 hours. It allows us to fabricate the low-loss Y-branching power dividers, utilizing a Y-branching (section II in Fig.1) formed by three single-mode channel waveguides (sections I and III, Fig.1). Besides, application of these fabrication parameters allow to obtain the low propagation losses[6] for straight and bended channel waveguides, and to avoid the marked degradation of electro-optic coefficients.

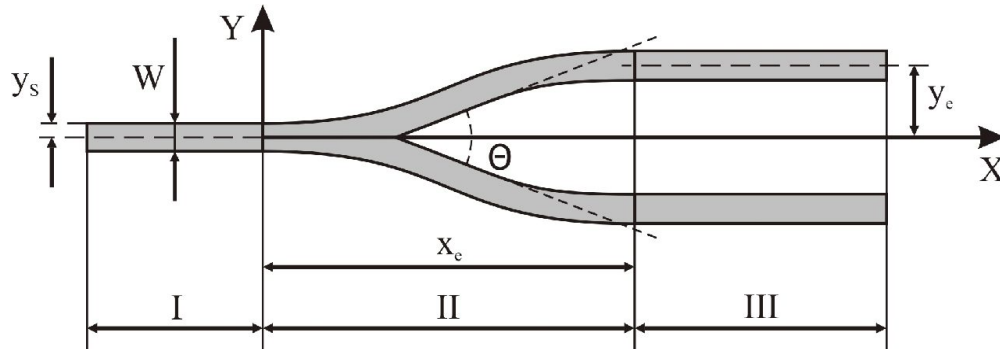[1] skostritskii@optolink.ru; phone +7-495-6631760-103; fax +7-495-6631761; www.optolink.ru

Figure 1. Layout of the Y-branching power divider. Θ is branching angle, W is channel waveguide width.

The different geometries of Y-branching were used to fabricate the three different types of Y-branching power divider for further comparative study, aiming to find geometry. The most reliable geometries for MIOC design are found to be described by the following equations:

$$y(x) = y_S + \frac{y_e - y_S}{x_e} \cdot x \tag{1}$$

$$y(x) = y_S + \frac{y_e - y_S}{x_e} \cdot x - \frac{y_e - y_S}{2\pi} \cdot \sin\left[\frac{2\pi}{x_e} \cdot x\right] \tag{2}$$

$$y(x) = y_S + \frac{y_e - y_S}{2} \cdot \left(1 - \cos\left[\frac{2\pi}{x_e} \cdot x\right]\right) \tag{3}$$

for so-called linear, sin and cosine branching, respectively. x_e is length of the branching section, y_e is deviation of output channel center from input channel center, $y_s = W/2$, Fig.1. The parameters x_e and y_e have values within the ranges of 7÷16 mm and 0.16÷0.2 mm, respectively. The width of tapered subsection of the section II near branching point is 2W.
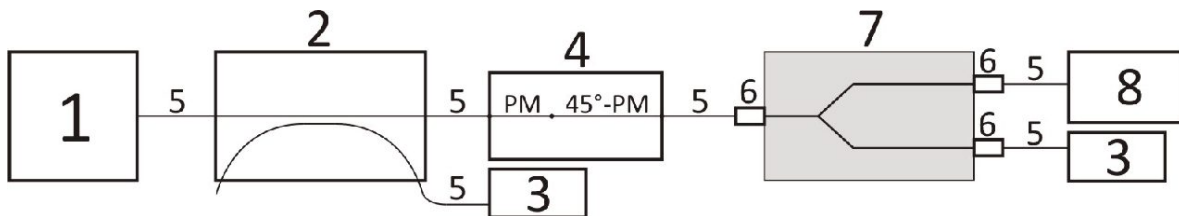

Figure 2. Experimental set-up, exploiting fiber-to-fiber coupling for input and output ports of MIOC: 1 – SLD; 2 – fiber splitter 1:10; 3 – photodiode; 4 - fiber Lyot depolarizer consisting of two segment of a PM fiber (PANDA type); 5 - isotropic SM fiber; 6 – pigtailing block; 7 – MIOC; 8 – OSA.

The main parameters of MIOCs were measured by coupling depolarized light into the waveguides with the aid of an isotropic single mode fiber. A fiber Lyot depolarizer utilizing polarization maintaining (PM) fiber was used to decrease sharply the degree of residual polarization of a superluminescent diode (SLD) radiation (central wavelength is ~1540 nm) and, hence, minimize a polarization-dependent error in measurement results. To determine insertion losses and splitting ratio, we use a fiber-to-fiber coupling set-up, Fig. 2. One input and two output ports of a MIOC were pigtailed by an UV-curied adhesive with a single-mode fiber, whish was adjusted accurately to provide a maximum coupling with channel waveguides and, hence, minimum insertion loss. The IR-radiation from the output ports of Y-branching power

divider was directed into a photodiode, operating in its linear region. Spectral dependence of output power at each output ports was measured with the aid of an optical spectral analyzer YOKOGAWA AQ6370.

3.   EXPERIMENTAL RESULTS AND DISCUSSION

The power transfer coefficient (PTC) is established to be critical parameter of the Y-branching, as this parameter is most sensitive to the variations in Y-branching topology and fabrication conditions[7]. PTC is evaluated experimentally as ratio between smaller output power, P'_{out}, and sum of both output powers:

$$PTC = P'_{out}/(P'_{out} + P''_{out}) \qquad (4)$$

i.e., PTC is directly related to a splitting ratio that is main parameter characterizing performance of the power divider. A perfect Y-branching power divider should have PTC = 0.5, and deviation of actual PTC averaged over entire spectrum of a light source (it's a broad-band SLD in our case) from this value is caused by parasitic asymmetry of Y-branching section due to technological imperfections and modes interaction, as this branching section may be regarded as analog of the directional coupler with weighted coupling[7,8], i.e. for normalized deviation parameter should be valid the following relation (see Fig. 3):

$$(0.5 - PTC) \sim \Delta\beta/\theta\gamma_3 \qquad (5)$$

where $\Delta\beta$ is accidental asymmetry of Y-branching caused by technological imperfections, Θ is branching angle, γ_3 is transverse component of phase constant, giving the strength of local normal mode coupling.
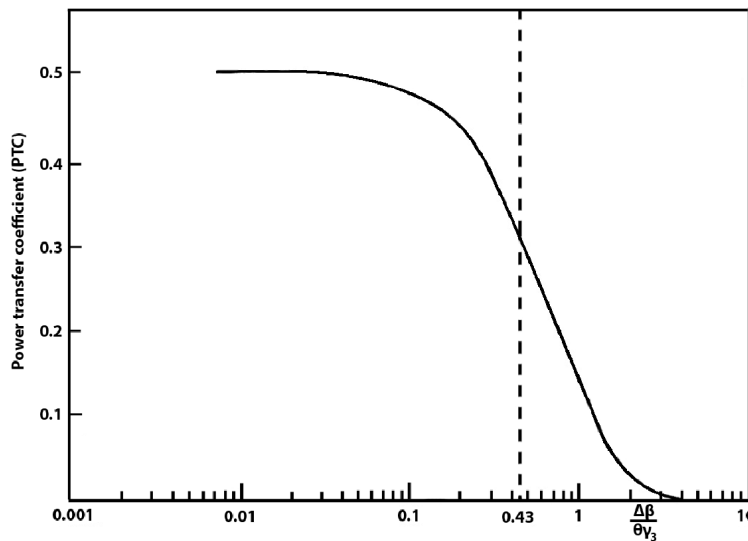

Figure 3. PTC versus parameter $\Delta\beta/\theta\gamma_3$ of mode coupling[7], for $\Delta\beta/\theta\gamma_3 > 0.43$ Y-branching acts as a mode splitter; <0.43 as a power divider.

Theoretically, the truncated tip of the waveguides branching (section II, Fig.1) is considered to be null. In practice, resulting from technological process limitations it is typically of the order of one micrometer[4,5], and a size and position of this tip, as well as initial section of "barrier" between two output channel waveguides, are not reproducible, that provides inherent character of the accidental asymmetry $\Delta\beta$. According to the theory of Y-branching[7], the shaped branching (2,3) has a resulting length advantage over the linear branching (1). To reach an appropriate value of PTC near 0.5, the branching angle should be large enough to decrease sufficiently the mode coupling. However the insertion losses represent the important limiting factor for further improvement of Y-branching via Θ increase.

In fact, the following statement may be derived from experiments with the Y-branching power dividers based on APE LiNbO$_3$ waveguides: a larger value of Θ is higher insertion loss for the power dividers of any studied geometry (1-3). At the same, the cosine branching (3) provides a smallest insertion loss among the geometries studied at any fixed value of Θ. Thus, optimisation of Y-branching power divider should find the compromise between smaller PTC and higher losses via choice of geometry and fabrication conditions providing appropriate values of both parameters. Simulation with the aid of the beam propagation method shows that the cosine branching (3) with average branching angle $\Theta = 1.4°$ is the optimal geometry, as it allows obtain the branching loss (α_b) about 0.3 dB at PTC ≤ 0.485. Our experimental study confirms this theoretical finding. However, the very strong parasitic spectral selectivity is observed for output of MIOC, which utilize this Y-branching geometry, Fig.4 (3). It has been attributed to the inherent asymmetry of Y-branching region, appearing due to technological uncertainty of photolithography and etching processes. Application of the other functions[4,5,7,8] of shaped Y-branching requires much fine tolerance for both these processes. Besides, some extra efforts, such as refractive index trimming in XY-plane (Fig.1), will be necessary. Therefore, these functions were not regarded in our present study.
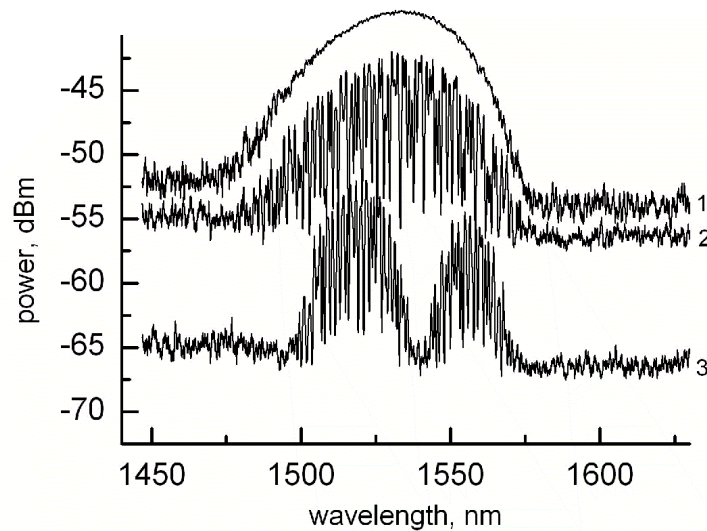

Figure 4. Spectral dependence of the power of IR radiation: (1) at SLD output fiber, (2) at output pigtail of straight channel waveguide (channel width W = 6.0 μm), (3) at output port of Y-branching power divider with cosine geometry (see Eq.(2)) and branching angle Θ is 1.4°. The power at second output port has spectral dependence oscillations of opposite sign. Thus, PTC varies from 0 to 0.5 within spectral band of SLD. To avoid spectra overlapping, curve 3 is shifted for -10 dBm relative to curves 1 and 3.
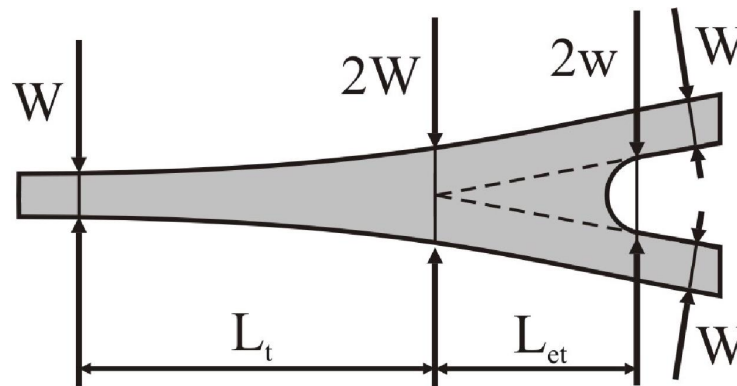

Figure 5. Topology of branching region: L_t – taper length, L_{et} and $2w$ – length and width of extra taper. Dashed lines show Y-branching without extra taper.

To suppress this parasitic effect, the extra taper (Fig.5) has been introduced into section II of the Y-branching power dividers in order to decrease the influence of technological uncertainty on mode coupling within initial stage of channel branching, due to a sharp decrease of $\Delta\beta$. This modification of Y-branching geometry gives the only partial suppression of the spectral selectivity (see Fig.6(1)), when appropriate levels of PTC and losses is obtained with growth of length and width of this extra taper.

Note, that even such a small wavelength-selective variation of PTC may present a dramatic problem for some particular applications, e.g. high-precision FOG[1,3]. To minimize the spectral selectivity, the branching angle Θ should be increased, as it should reduce an absolute value of the mode coupling strength within the branching region (representing a coupler with weighted coupling[7,8]) as well as the wavelength dependence of this coupling strength. However, a branching loss (α_b) must grow at such an increase[3,9] of Θ. Thus, $\Theta = 1.9°$ is evaluated as the optimal value for the cosine-branching (3) with extra taper of $L_{et} = 100$ μm, $2w = 1.18$ μm and $W= 6$ μm, when $\alpha_b = 0.6$ dB, Fig. 6(2). This finding has been verified experimentally, as the numerous series of lithium niobate substrates, containing the power dividers with different Y-branching topologies, were treated by APE technique. It is important to note, that these quantitative estimations may be used only for optimization of the Y-branching power dividers fabricated by APE technique in lithium niobate, as mode coupling within the branching region has been established to be quantitatively different comparative to the dividers fabricated by Ti-indiffusion technique[7].
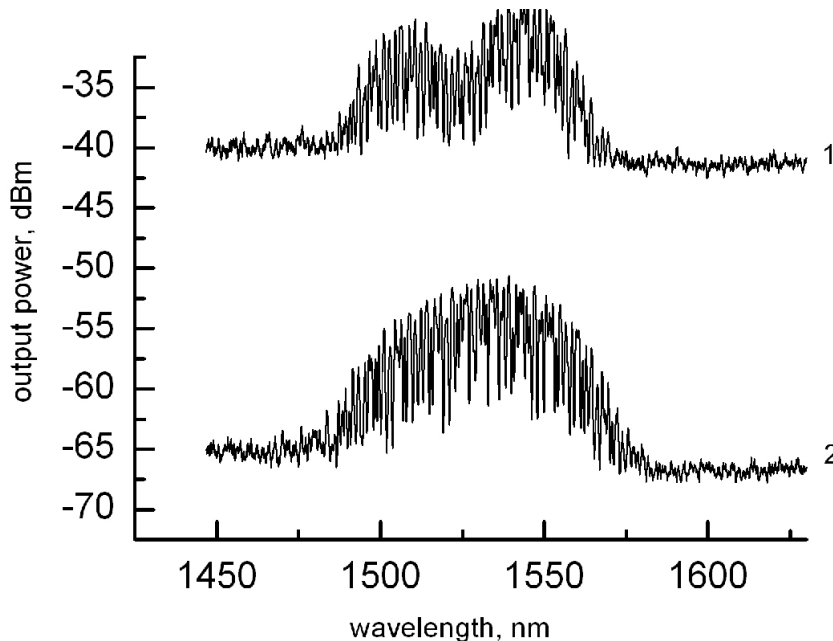

Figure 6. Spectral dependence of the power of IR radiation at output port of Y-branching power divider with cosine topology and the extra taper introduced in branching region (see Fig.3): (1) $\Theta =1.4°$ and the extra taper has $L_{et} = 130$ μm and $2w = 1.26$ μm, (2) $\Theta = 1.9°$, $L_{et} = 100$ μm and $2w = 1.18$ μm. To avoid overlapping, curve 2 is shifted for -24 dBm relative to curve 1.

Moreover, such an increase of the branching angle Θ has been found to be effective to suppress influence of the photorefractive damage (PRD) on performance of Y-branching power dividers[3]. For example at high input powers (>100 mW), some MIOCs, that have a pronounced parasitic spectral selectivity, were observed to undergo asynchronous, oscillatory power exchange between outputs with response time specific for photorefractive effect[3]. PRD is a well-known classical problem for most electro-optic and nonlinear optic applications of $LiNbO_3$ crystals: Optically induced change of refractive index creates difficulties to produce stable devices in this material for visible and near IR ranges. This problem is most dramatic in case of integrated-optical (IO) devices, utilizing channel waveguides, due to the following specific features:

1)- Light beams are confined in two dimensions to region only a few micrometers in size and very high optical intensities are thus obtained even at small input powers;

2)- The inhibition of diffraction leads to effects, which do not occur in bulk samples;

3)- Waveguide fabrication means heavy doping, as industrial IO $LiNbO_3$ devices are fabricated only by the two techniques: Ti-indiffusion or proton exchange. Therefore, the IO $LiNbO_3$ circuits must be designed so that effects of the photorefractivity are adequately compensated and knowledge of photorefractive properties is required in developing advanced devices. However, further increase of Θ, L_{et} and 2w is out of practical interest, as it will induce sharp growth of α_b. Note, that the cosine Y-branching power divider (3) with the same Θ but with a much smaller extra taper (i.e., when values of L_{et} and 2w are decreased comparative to the mentioned above optimal values), including the case of extra taper absence, demonstrates marked parasitic spectral selectivity.

4. SUMMARY

A dramatic oscillating spectral dependence of power transfer coefficient for the proton-exchanged $LiNbO_3$ MIOCs consisting of a standard Y- branching power divider was observed at application of a broadband SLD with the central wavelength about 1540 nm. Fabrication conditions and branching topology allowing for suppression of such a parasitic spectral selectivity of Y-branching power dividers have been identified. The low-loss spectral-insensitive MIOCs, operating within wavelength range of 1510 to 1580 nm were fabricated. Besides, the modified Y-branching geometry with an increased branching angle (near 1.9[o]) and rather long extra taper (80-130 μm) is determined to be most suitable for high-power application, as MIOC becomes rather stable to parasitic influence of photorefractive damage.

REFERENCES

[1] Lefevre, H., [The Fiber-Optic Gyroscope], Artech House Inc, Boston & London, 43-55 (1993).

[2] Kostritskii, S. M., Korkishko, Yu. N., Fedorov, V. A., Alkaev, A. N., Kritzak, V. S., Moretti, P., Tascu, S. and Jacquier, B., "Leakage of a guided mode caused by static and light-induced inhomogeneities in channel HTPE-$LiNbO_3$ waveguides", Proc. SPIE 4944, 346-352 (2003).

[3] Kostritskii, S. M., "Photorefractive effect in $LiNbO_3$-based integrated optical circuits at wavelengths of third telecom window", Applied Physics B 95, 421-428 (2009).

[4] Wang, Q., He, S. and Wang, L., "A low-loss Y-branch with a multimode waveguide transition section", IEEE Photonics Technology Letters 14 (8), 1124-1126 (2002).

[5] Hauden, J., Grossard, N. and Porte, H., "Ultra low loss split Y-junctions: Application to QPSK-lithium niobate modulators", 15th European Conference on Integrated Optics (ECIO'2010), Cambridge, UK, April 07-09, 2010, paper ThP30.

[6] Howerton, M. M., Burns, W. K., Skeath, P. R. and Greenblatt, A. S., "Dependence of refractive index on hydrogen concentration in proton exchanged $LiNbO_3$", IEEE Journal on Selected Topics in Quantum Electronics, 27, 593-600 (1991).

[7] Burns, W. K. and Milton, A. F., "Waveguide transitions and junctions", [Guided-wave optoelectronics], T. Tamir (ed.), Springer-Verlag, Berlin & Hiedelberg, 89-144 (1988).

[8] Nishihara, H., Haruna, M. and Suhara, T., [Optical integrated circuits], McGraw-Hill Book Company, New York, 246-256 (1985).

[9] Sakamaki, Y., Saida, T., Hashimoto, T., Takahashi, H., "Low-Loss Y-branch Waveguides Designed by Wavefront Matching Method", IEEE Journal of Lightwave Technology 27(5), 1128 – 1134 (2009).